

Joule heating and high frequency nonlinear effects in the surface impedance of high T_c superconductors

Julien Kermorvant,¹ Cornelis Jacominus van der Beek,² Jean-Claude Mage¹, Bruno Marcilhac,¹ Yves Lemaître,¹ Javier Briatico,¹ Rozenn Bernard,¹ Javier Villegas¹

¹ Unité Mixte de Recherche en Physique UMR 137 CNRS-THALES and

² Laboratoire des Solides Irradiés, CNRS-UMR 7642 & CEA-DSM-IRAMIS,
Ecole Polytechnique, F 91128 Palaiseau cedex, France

Abstract

Using the dielectric resonator method, we have investigated nonlinearities in the surface impedance $Z_s = R_s + jX_s$ of $\text{YBa}_2\text{Cu}_3\text{O}_{7-\delta}$ thin films at 10 GHz as function of the incident microwave power level and temperature. The use of a rutile dielectric resonator allows us to measure the precise temperature of the films. We conclusively show that the usually observed increase of the surface resistance of $\text{YBa}_2\text{Cu}_3\text{O}_{7-\delta}$ thin film as function of microwave power is due to local heating.

PACS numbers: 74.25.NF; 74.25.OP; 74.78.BZ

Keywords: Microwave nonlinearities; Surface impedance; High Tc superconductors

I. INTRODUCTION

High Temperature Superconductor (HTSC) films are suitable candidates for the improvement of microwave receiver performance because of their low surface resistance.^{1,2,3,4} The surface impedance of HTSC materials presents a strong dependence on the magnitude of the incident microwave magnetic field, H_{rf} . Typically, a nonlinear behavior is observed above a certain value of H_{rf} . This nonlinearity leads to unacceptable microwave power losses. Microwave losses are characterized by a decrease of the quality factor Q of superconducting resonators and filters and a downward shift of the resonant frequency of the former.^{5,6,7} The surface impedance of HTSC has been studied by many groups, using either the dielectric resonator technique or the stripline resonator technique. In spite of numerous experimental studies the physical origin of the observed nonlinearities is still under debate and the subject of present-day experimental investigation.^{8,9,10,11,12}

It has been proposed that a simple way to differentiate among the mechanisms of nonlinearity of the surface impedance is the examination of the r parameter.¹³ This quantity is defined as the ratio between the microwave field dependence of the surface reactance $\Delta X_S(H_{rf})$ and of the surface resistance $\Delta R_S(H_{rf})$,

$$r = \frac{\Delta X_S(H_{rf})}{\Delta R_S(H_{rf})}. \quad (1)$$

Table 1 gives an overview of possible mechanisms leading to the nonlinear behavior of the surface impedance.^{14,15,16} First is the intrinsic nonlinearity due to pair-breaking. The nonlinearity is then related to the increase of the quasi-particle density n_{qp} ^{17,18} when the H_{rf} -induced current density is of the order of magnitude of the pair-breaking current density. A nonlinearity based on this effect has been predicted and investigated using a phenomenological expression for a nonlinear penetration depth. If the nonlinearity is dominated by this intrinsic mechanism, the r -parameter should be small and strongly frequency-dependent. This differs from the experimentally observed nonlinearities. Hysteretic losses are also proposed to be significant.^{19,20,21} The weakly coupled-grain model holds that the large surface resistance of highly granular high- T_c superconductors as compared to single crystals can be explained by the different morphology. The polycrystalline samples can be modeled as a network of Josephson junctions. Nonlinear behavior is expected at rf-current densities that are limited by critical current density of the constituent Josephson junctions. This model

yields a very small r -parameter with a strong dependence on temperature and frequency. In the case of granular films the coupled-grain model describes the microwave nonlinearities fairly well. Nevertheless, it fails to describe strong nonlinearities in epitaxial films. Vortex penetration and creep into grain boundaries and/or weak links are also proposed as a possible source of microwave hysteretic losses. Vortex generation by the microwave magnetic field has been predicted^{22,23,24} and the Bean model has been extended to account for microwave nonlinearity in HTSC films. The dependence of R_s on X_s is almost linear (with slope r). Experimental values are close to those predicted by the model. The last possible effect to explain nonlinearity is local or uniform heating.^{25,26,27,28} It has been proposed that heating can occur in superconducting thin films. This effect appears in the microwave frequency range, particularly in continuous mode, but also in pulsed mode, as function of the pulse period. Heating is significant above a certain value of the incident microwave power, and causes the transition to the normal state of weaker superconducting regions such as weak links or local defects. Heating and heat transfer to the substrate are shown to play an important role.

We have used the dielectric resonator method in order to measure the surface impedance of $\text{YBa}_2\text{Cu}_3\text{O}_{7-\delta}$ thin films from various sources. We present a study of both the temperature and the microwave power level dependence. The use of a rutile dielectric resonator allows us to measure the precise temperature of the films. We show that the usually observed increase of the surface resistance of $\text{YBa}_2\text{Cu}_3\text{O}_{7-\delta}$ thin films as a function of microwave power is due to local heating.

II. EXPERIMENTAL DETAILS

Measurements of the surface impedance $Z_s = R_s + jX_s$ were performed on a series of $\text{YBa}_2\text{Cu}_3\text{O}_{7-\delta}$ thin films, denoted SY211 and obtained at THALES by inverted cylindrical hollow cathode dc sputtering. A second series, labelled TM MgO and TM LAO, was acquired from THEVA Inc.²⁹ This series was prepared by reactive thermal evaporation. Z_s was measured by the dielectric resonator method.^{30,31,32,33,34} The film thicknesses and the critical temperatures as measured by ac-susceptibility are gathered in Table 2. Surface morphology imaging is shown in Fig. 1 for the three studied samples. X-ray diffraction, using a Bragg-Brentano diffractometer, showed all films to be epitaxial with the [001] orientation.

For the surface impedance measurements, we have used a cylindrically shaped rutile resonator of height 1 mm and diameter 7 mm, which is directly placed onto the sample. The resonant frequency in the TE_{011} mode is near 10 GHz. Rutile is well-known for its small tangent loss ($\tan \delta = 10^{-5}$ at 77 K, 10 GHz) and its very high dielectric constant ($\epsilon = 105$ at 77 K).^{35,36} The resonator is excited by an adjustable coupling loop; the distance between the resonator and the loop is controlled in order to maintain critical coupling during the experiment. The whole assembly is placed inside an oxygen-free high conductivity copper cavity, mounted onto a cryocooler cold head. Temperature stability is better than 1 mK over the range 30 K-90 K.

For each sample, we measure the resonant frequency f_0 and the loaded Q -factor of the fundamental resonance of the resonator. At each microwave input power level, the reflection coefficient from the resonator, or S_{11} parameter, is measured with a network analyser in continuous mode, coupled to a microwave amplifier for the high power regime. This experimental set-up allows us to measure the surface impedance over a input microwave power ranging from 0.01 mW to 100 mW.

The loaded Q -factor of the resonator is given by:

$$Q_L = \frac{f_0}{\Delta f}, \quad (2)$$

where f_0 and Δf are, respectively, the resonant frequency and the -3 dB bandwidth in log scale corresponding to the resonant peak, see Fig. 2.

The unloaded Q -factor is defined by :

$$Q_0 = (1 + \beta)Q_L, \quad (3)$$

with β the coupling constant. All measurements were performed under critical coupling *i.e.* $\beta = 1$, and the unloaded Q -factor $Q_0 = 2Q_L$. The inverse Q_0^{-1} is the sum of different contributions due to the resonator itself, the copper cavity, and the $\text{YBa}_2\text{Cu}_3\text{O}_{7-\delta}$ thin film, such that

$$\frac{1}{Q_0} = \frac{1}{Q_{\text{resonator}}} + \frac{1}{Q_{YBCO}} + \frac{1}{Q_{Cu}}. \quad (4)$$

Here $Q_{\text{resonator}}^{-1} = A \tan \delta_{TiO_2}$ is due to the dielectric losses, $Q_{Cu}^{-1} = CR_{s,Cu}$ to the microwave losses in the copper, and $Q_{YBCO}^{-1} = BR_{s,YBCO}$ arises from the microwave losses in the

$\text{YBa}_2\text{Cu}_3\text{O}_{7-\delta}$ film. The geometrical factors $A=0.9871$, $B=1.75 \cdot 10^{-2}$, $C=3.665 \cdot 10^{-5}$ are calculated using a numerical simulation (HFSS software³⁷).

The surface resistance is obtained as

$$R_{s,YBCO} = \frac{1}{B} \left(\frac{1}{Q_0} - A \tan \delta_{TiO_2} - C R_{s,Cu} \right). \quad (5)$$

III. RESULTS

In order to understand the variation of the Q -factor and the resonant frequency with increasing microwave power, we have measured the temperature dependence of the resonator's properties. Fig. 3(a) represents the temperature dependence of the TiO_2 resonator resonant frequency in the limit of small microwave power P_{rf} , for three different configurations. In the first configuration, the TiO_2 resonator is directly placed on the copper cavity; in the second, the resonator is placed on an MgO substrate; finally the resonator is placed on the $\text{YBa}_2\text{Cu}_3\text{O}_{7-\delta}$ film, itself deposited on MgO . The absolute value of the resonant frequency, f_0 , depends on the distance between the resonator and the conducting wall of the copper cavity or of the superconducting layer. The presence of dielectric MgO leads to a lower resonant frequency than the presence of the conducting $\text{YBa}_2\text{Cu}_3\text{O}_{7-\delta}$ layer. However, the temperature dependence of the frequency shift of the rutile resonator does not depend on the nature of the support. This shows that the thermal conductivity between the cryocooler cold-head and the rutile resonator is not significantly affected by the intercalation of the 500 μm -thick MgO and the 400 nm-thick superconducting layer.

Fig. 3(b) represents the temperature dependence of the resonant frequency shift of the rutile resonator and of a MgO resonator with f_0 near 8 GHz. Clearly, the variation with temperature of the MgO resonant frequency is much weaker than that of rutile. The temperature dependence of the resonant frequency is the direct consequence of the increase (resp. decrease) with temperature of the dielectric constant $\epsilon(T)$ of rutile (resp. MgO).

In Fig. 4 (a,b) we present the surface resistance and the resonant frequency in the presence of the investigated $\text{YBa}_2\text{Cu}_3\text{O}_{7-\delta}$ films at a given temperature of 74 K, as function of an effective microwave reactive power. This is defined by $\tilde{P}_{rf} = P_{\text{incident},rf} \times Q_L$, a parameter introduced to quantitatively compare data obtained on the different films. Namely, each different film leads to a different values of Q_L and absorbed power for the same incident

microwave power. The zero power limit is taken as those values of \tilde{P}_{rf} below which $R_s(\tilde{P}_{rf})$ is essentially \tilde{P}_{rf} -independent. Curves for different films present the same behavior, *i.e.* $R_s(\tilde{P}_{rf})$ and $f_0(\tilde{P}_{rf})$ are independent of the microwave field in the zero field limit and become nonlinear (increase rapidly) above a threshold value \tilde{P}_{rf} .

Contrary to what is expected and usually observed by using sapphire or MgO resonators, the resonant frequency f_0 of the rutile resonator also increases with increasing microwave power. We ascertain that the increase of $f_0(\tilde{P}_{rf})$ is due to the heating of the rutile resonator by the $\text{YBa}_2\text{Cu}_3\text{O}_{7-\delta}$ film. In order to demonstrate this effect, we have also measured the temperature dependence of the surface resistance and resonant frequency in the limit of small \tilde{P}_{rf} . The surface resistance at $\tilde{P}_{rf} \rightarrow 0$ of the $\text{YBa}_2\text{Cu}_3\text{O}_{7-\delta}$ films, shown by the open symbols in Fig. 5(a), shows the usual monotonous increase with temperature for all samples. Concerning the temperature dependence of the resonant frequency, we observe an increase with temperature, as discussed previously, Fig. 5(b). The only observed difference is the nearly constant frequency offset between the three curves.

By fitting the $T(f_0)$ curve of Fig. 5(b) and substituting the interpolated values for the f_0 -values measured in the swept-power experiment depicted in Fig. 4(b), we estimate the temperature variation $T(\tilde{P}_{rf})$ of the resonator in the latter. Fig. 6 shows the temperature variation of the resonator obtained in this way, at nominal temperatures of 63 K (a) and 74 K (b). Fig. 7 shows the normalized resonant frequency f_0 of the rutile resonator placed on a superconducting layer (black square) and on a MgO substrate (black star) as a function of the microwave reactive power. This graph shows that the contribution to the observed nonlinearities arising from the losses in the dielectric material is negligible compared to the losses in the superconductor.

We now compare the R_S data obtained as function of the temperature increase due to increasing dissipation in the swept-power experiments and the low-power $R_S(T)$ data. Fig. 5(a) shows a superposition of $R_S(T)$ obtained from swept-power experiments at nominal temperatures of 63 K and 74 K (Fig. 6 closed symbols) and the low-power $R_S(T)$ data (open symbols). The data are perfectly superimposed, this means that no intrinsic \tilde{P}_{rf} -dependence of the surface resistance is measured, and that any observed nonlinearity is the consequence of Joule heating.

IV. DISCUSSION

The temperature dependence of the resonant frequency is the direct consequence of the increase with temperature of the dielectric constant $\epsilon(T)$ of rutile. Note that its behavior is opposite to the decrease with temperature of the dielectric constant of more commonly used sapphire or MgO resonators. Moreover, the variation with temperature of the MgO resonant frequency is much weaker than that of rutile. By consequence, it is difficult to separate the evolution of the intrinsic change of a MgO or sapphire resonator's frequency from that caused by the temperature variation of a superposed superconducting film: both weakly decrease as function of temperature. However, the intrinsic evolution of the rutile resonator's frequency is opposite to that expected from the presence of the superconducting film. A measurement of the rutile's resonator frequency can thus unambiguously serve as a local temperature measurement.

In general, superconducting thin films contain resistive defects such as conducting precipitates and weak-links of Josephson junctions. In their experiments, Obara et al.³⁸ show a correlation between the H_{rf} -dependence of the surface resistance and the value of the dc critical current density. Their interpretation is these correlations indicate that the power dependence of R_s is due to the intrinsic properties of the films, such as pair-breaking. However, nonlinearities usually occur at much lower H_{rf} fields than those at which the intrinsic nonlinearities are expected.^{39,40,41,42} Halbritter et al.⁴³ show that at very low microwave fields, nonlinearities can be explained by Josephson fluxon penetration along weak links; at higher fields flux flow losses may also participate.⁴⁴ Wosik et al. insist on the importance of thermal effects as the root of the nonlinear behavior.^{45,46,47} They have used the pulsed measurement method, which, in principle, prevents or at least reduces heating of the films. These experiments were repeated using thermally isolated films as well as films that are thermally connected through the substrate with the heat sink cooled at 20 K. The authors^{45,46,47} have shown that the temperature increase of an isolated sample can reach 30 K. For the case of a film thermally connected to the heat sink the temperature rise will be of only 2.5 K.

V. CONCLUDING REMARKS

In our experiment we have clearly shown that the use of the rutile dielectric material is a good way for a direct measurement of the temperature of superconducting thin films, because of the large temperature dependence of the dielectric constant. The behavior of the resonant frequency, opposite to that of the commonly used sapphire or MgO resonators, indicates that the resonant frequency shift observed as function of the applied microwave power is mainly due to heating of superconducting films. The perfect superposition of the temperature-dependent surface resistance obtained from swept-power experiments with the temperature dependence of R_s measured in the limit of low microwave power shows that intrinsic nonlinearities of the superconducting films do not contribute to heating. Therefore, Joule heating must be due to either flux-flow losses or to quasi-particle resistive losses.

-
- ¹ Hein M.A in 'Studies of high temperature superconductors' V.18 ed. by A.Narlikar, (Nova, NY 1996) 11-216
- ² Gallop J, 1997 *Supercond. Sci. Technol.* **10** 120
- ³ Portis A.M 'Electrodynamics of high temperature superconductors' Lecture Notes in Physics, V.48 '(World scientific, Singapore) 1993
- ⁴ Lancaster M.J, Passive Microwave Device Applications of High temperature superconductors (Cambridge University Press, 1997)
- ⁵ Samoilova T.B 1995 *Supercond. Sci. Technol.* **8** 259
- ⁶ Schen Z.Y and Wilker C, 1994 Microwave and RF p.129
- ⁷ Hein M, Diete W, Getta M, Hensen S, Kaiser T, Müller G, Piel H and Schilck H 1997 *IEEE Trans. Appl. Supercond.* **7** 1264
- ⁸ Lee J.H, Yang W.I, Park E.K and Lee S.Y 1997 *IEEE Trans. Appl. Supercond.* **47** 2
- ⁹ Wosik J, Xie L.M, Maziera and Grabovickic 1999 *Appl. Phys. Lett* **75** 12
- ¹⁰ Nguyen P.P, Oates D.E, Dresselhaus G and Dresselhaus M.S 1993 *Phys. Rev.B* **51** 10
- ¹¹ Hein M, Kaiser T and Muller G 2000 *Phys. Rev. B* **61** 1
- ¹² Xin H, Oates D.E, Anderson A.C, Slattery R, Dresselhaus G, and Dresselhaus M.S 1999 *arXiv:cond-mat/9906044 v1*
- ¹³ Herd S, Oates D.E and Halbritter J 1997 *IEEE Trans. on Appl. Supercon.* **7** 2
- ¹⁴ Lahl P and Wördnenweber R 2004 *Supercond. Sci. Technol.* **17** 369-374
- ¹⁵ Oates D.E, Hein M.A, Hirst P.J, Humphreys R.G, Koren G and Polturak E 2002 *Physica C* **372-376** 462-468
- ¹⁶ Golosovsky M 1998 *Particle Accelerator* **351** 87
- ¹⁷ Dahm T and Scalapino D.J 1996 *Appl. Phys. lett.* **69** 4248
- ¹⁸ Dahm T and Scalapino D.J 1997 *Appl. Phys. lett.* **81** 2002
- ¹⁹ Hylton T.L et al 1998 *Appl. Phys. Lett* **53** 1343
- ²⁰ Hylton T.L and Beasley 1989 *Phys. Rev.B* **39** 9042
- ²¹ Dimas D et al 1990 *Phys. Rev. B* **41** 4038
- ²² Dahm B et al 1999 *Nature* **399** 439
- ²³ Sridhar S et al. 1994 *Appl. Phys. Lett* **65** 1054

- ²⁴ McDonald J, Clem J.R and Oates D.E 1997 *Phys. Rev.B* **55**, 11823
- ²⁵ Hein M 1999 *Springer Tracts in Modern Physics* **155**, Springer-Verlag
- ²⁶ Wosik J, Xie L.M, Nesteruk K, Li D, Miller J.H and Long S 1997 *Journal of Superconductivity* **10** 2
- ²⁷ Pukhov A.A et al. 1997 *Supercond. Sci. Technol.* **10** 82
- ²⁸ Pukhov A.A et al. 1997 *Supercond. Sci. Technol.* **12** 102
- ²⁹ Sample No X100707 4 THEVA Dünnenschichttechnik GmbH 85737 Ismaning Germany
- ³⁰ Hein M, Diete W, Getta M, Hensen S, Kaiser T, Müller G, Piel H and Schilck H 1997 *IEEE Trans. on Appl. Supercond.* **7** 2
- ³¹ Marzierska J 1998 *IEEE Trans. on Appl. Supercond.* **8** 4
- ³² Wilker C, Shen Z.Y, McKenna S.P, Carter C.F and Brenner M.S 2003 *Journal of superconductivity* **16** 5
- ³³ Lee J.H, Yang W.I, Kim M.J, Booth J.C, Leong K, Schima S, Rudman D and LEE S.Y 2005 *IEEE Trans. on Appl. Supercond.* **7** 2
- ³⁴ Diete W, Getta M, Hein M, Müller G, Piel H and Schilck H 1997 *IEEE Trans. on Appl. Supercond.* **8** 2
- ³⁵ Tobar M.E, Krupka J, Harnett J.G, Ivanov E.N and Woode R.A 1997 *IEEE international frequency control symposium*
- ³⁶ Mage J.C and Dieumegard D 1990 *AGARD Conference Proceeding No 481, Bath, U.K.*
- ³⁷ HFSS 3D Full-Wave Electromagnetic Field Simulation www.ansoft.com
- ³⁸ Obara H, Murugesan M, Develos-Bagarinao K, Mawatari Y, Yamasaki H and Kosaka S 2006 *Journal of Superconductivity and Novel Magnetism* **19** 7-8
- ³⁹ Nguyen P.P, Oates D.E, Dresselhaus G and Dresselhaus M.S 1993 *Phys. Rev.B* **48** 9
- ⁴⁰ Keskin E et al. 1999 *IEEE Trans. on Appl. Supercond.* **9** 2452
- ⁴¹ Gaganidze E et al. *1ME03 ASC 2000*
- ⁴² Halbritter J et al. 1995 *Journal of superconductivity* **8** 691
- ⁴³ Halbritter J, Numssen K and Gaganidze E 2001 *IEEE Trans. on Appl. Supercond.* **11** 1
- ⁴⁴ Gurevich A et al. 1993 *Phys. Rev. B* **48** 2857
- ⁴⁵ Wosik J, Xie L.M, Miller J.H and Long S 1997 *IEEE Trans. on Appl. Supercond.* **7** 2
- ⁴⁶ Wosik J, Xie L..M, Nesteruk K, Li D, Miller J.H and Long A 1997 *journal of superconductivity* **10** 2

⁴⁷ Wosik J, Xie L..M, Grabovickic R, Hogan T and Long S.A 1999 *IEEE Trans. on Appl. Supercond.* **9** 2

TABLE I: Possible mechanisms causing nonlinearity of the surface impedance.

Mechanism	Ref	R_s and X_s microwave field dependence	r value	Temperature dependence of r	Frequency dependence of r
Intrinsic non linearity [17-18]		$\propto H_{rf}^2$ low power	10^{-2}	Increase with T	$\propto \omega$
Pairbreaking		$\propto H_{rf}^4$ high power			
Weakly coupled grain [19-21]		$\propto H_{rf}^2$	10^{-3}	increase with T	$\propto \omega$
Vortices in weak link [22-24]		$\propto H_{rf}$	≤ 1	T independent	ω independent
Vortex penetration [22-24]		$\propto H_{rf}^n$ $n \sim 4$	const ~ 1	T independent	ω independent
		to the grains			
Uniform heating [25-28]		$\propto H_{rf}^2$	10^{-2}	increase with T	$\propto \omega$
Heating of weak link [25-28]		unknown	$\simeq 1$	T independent	ω independent

TABLE II: Basic properties of the studied samples.

Name	Substrate	Thickness(nm)	T _c (K)
SY211	MgO	400	88
TM MgO	MgO	700	88.5
TM LAO	LaAlO ₃	700	88.3

TABLE III: R_s and f_0 for $\tilde{P}_{rf} = P_{nl}$ at 74 K and in the limit of small power regime at $T = T_{nl}$.

name	\tilde{P}_{rf} (W)	$R_s(\tilde{P}_{rf} < P_{nl})$	$f_0(\tilde{P}_{rf} < P_{nl})$	T_{nl} (K)	$R_s(T < T_{nl})$	$f_0(T < T_{nl})$
SY211	110.81	474.37 $\mu\Omega$	9.9805 GHz	55.12	176.43 $\mu\Omega$	9.8735 GHz
TM LAO	135.26	302.34 $\mu\Omega$	9.9758 GHz	63.74	173.72 $\mu\Omega$	9.9187 GHz
TM MgO	137.75	236.99 $\mu\Omega$	9.9740 GHz	64.94	149.71 $\mu\Omega$	9.9284 GHz

FIG. 1: Scanning electron microscope images for the three studied samples

FIG. 2: Plot of the resonant peak of the rutile resonator on $\text{YBa}_2\text{Cu}_3\text{O}_{7-\delta}$ film at different microwave input power levels.

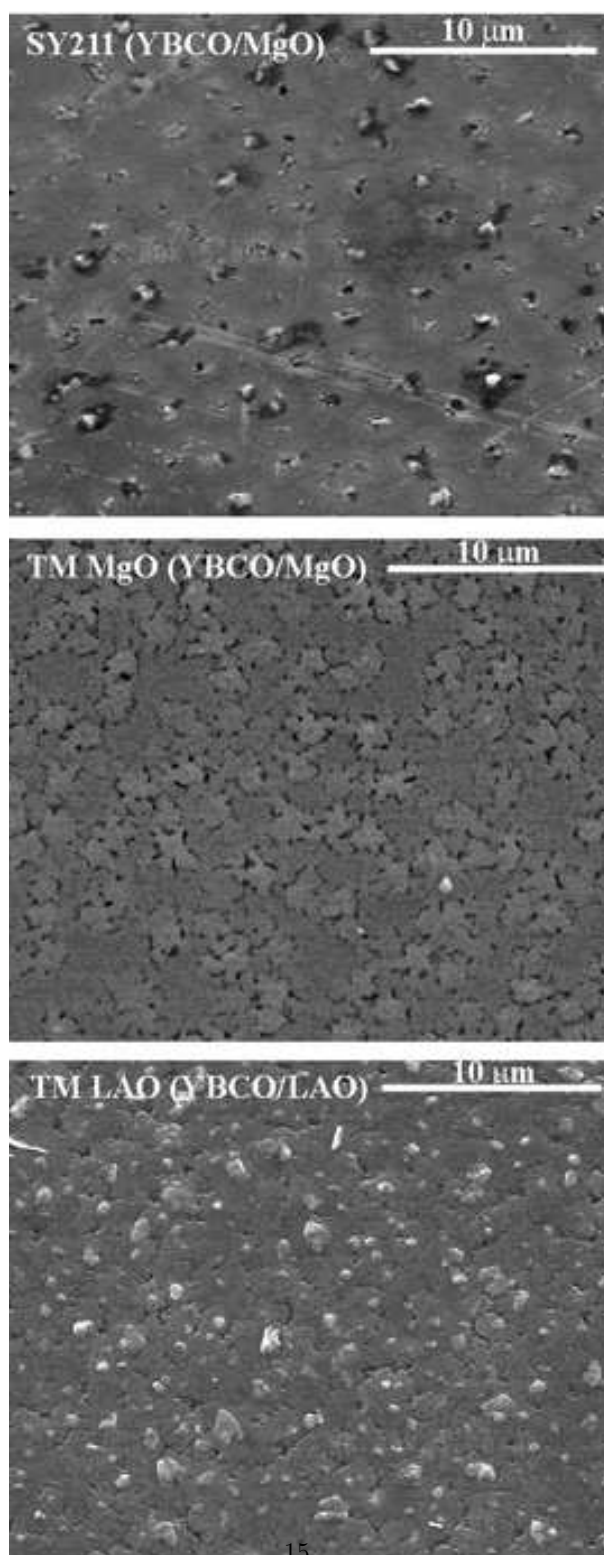
FIG. 3: (a) Plot of the resonant frequency of the TiO_2 resonator in three different configurations: Open squares: TiO_2 directly placed onto the copper cavity; closed stars: TiO_2 placed on an MgO substrate, itself placed in the copper cavity; open triangles TiO_2 placed on the superconducting layer deposited on MgO itself placed in the copper cavity. (b) Temperature dependence of the resonant frequency of the TiO_2 and MgO resonators.

FIG. 4: Dependence of the surface resistance (a) and of the resonant frequency (b) on microwave reactive power \tilde{P}_{rf} , at 74 K.

FIG. 5: Temperature dependence of the surface resistance (a). Open symbols denote the surface resistance as function of the directly measured temperature in the limit of small microwave power; closed symbols show the surface resistance measured in the swept-power experiment as a function of the calculated temperature. (b) The resonant frequency in the regime of low microwave power; the nearly constant offset between the three curves is due to the different values of the film and substrate thickness .

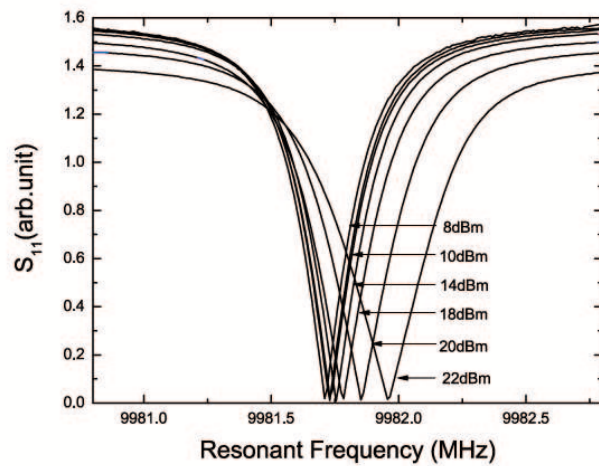
FIG. 6: Estimated temperature of the films, as deduced from the variation of the resonant frequency, as function of reactive microwave power, for a base (measurement) temperatures of (a) 63 K and (b) 74 K.

FIG. 7: Resonant frequency of the rutile resonator as function of the microwave reactive power with the resonator placed on a superconducting layer (Black square) and on an MgO substrate (Black star)

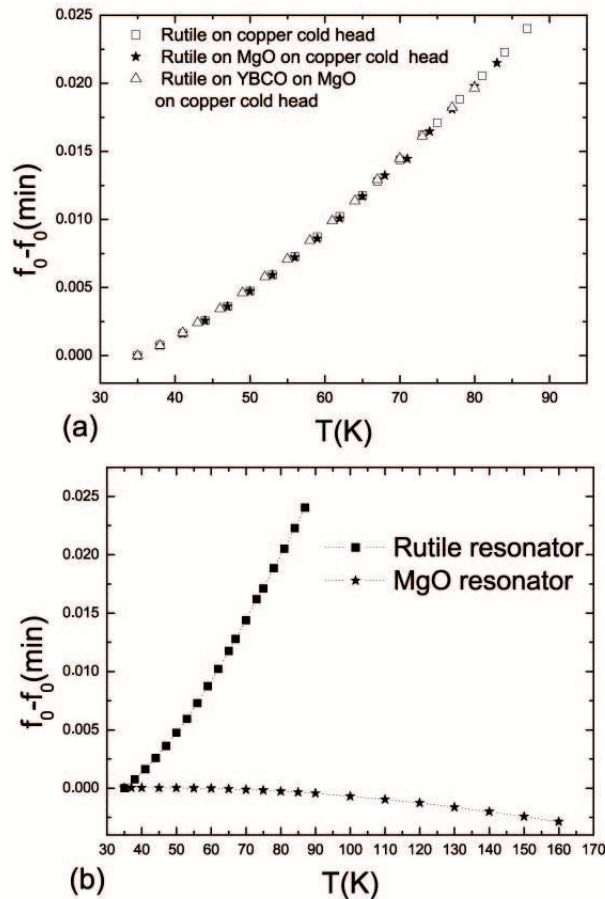


15

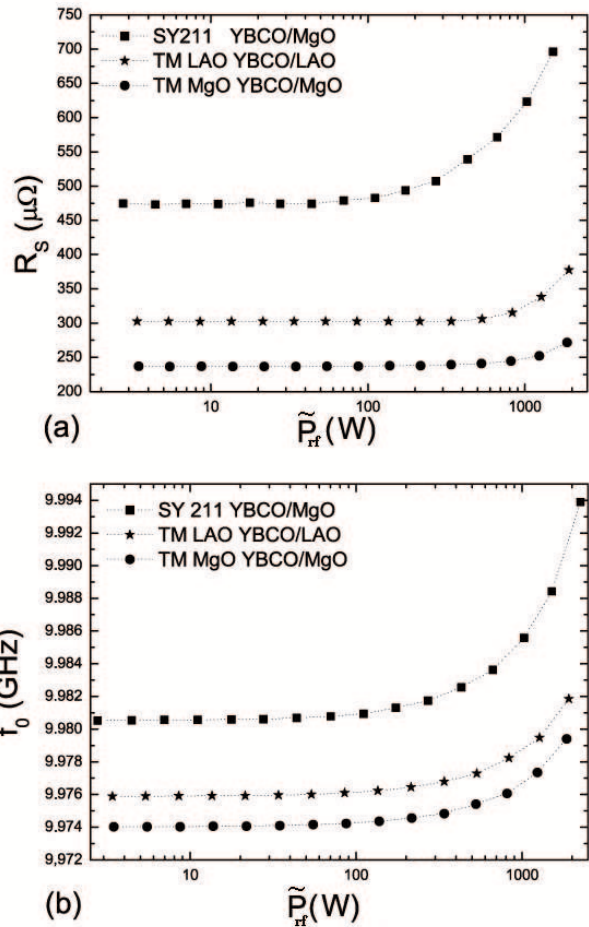
Kermorvant et al. Fig. 1



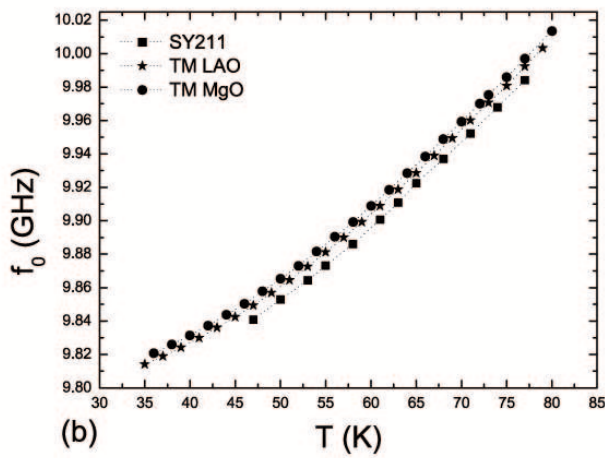
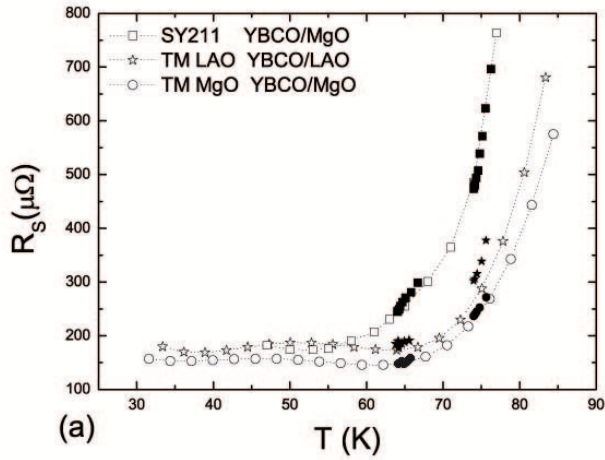
Kermorvant et al. Fig. 2



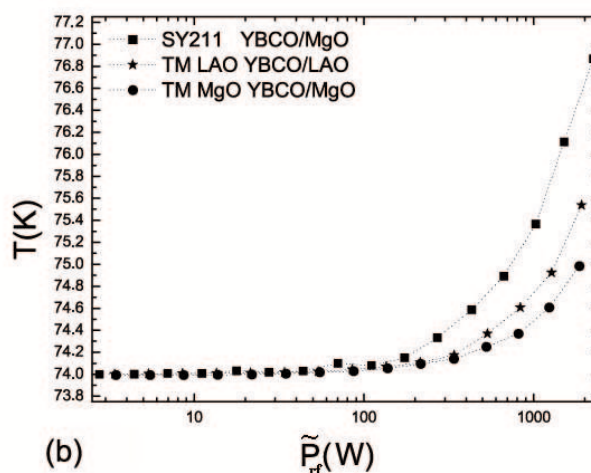
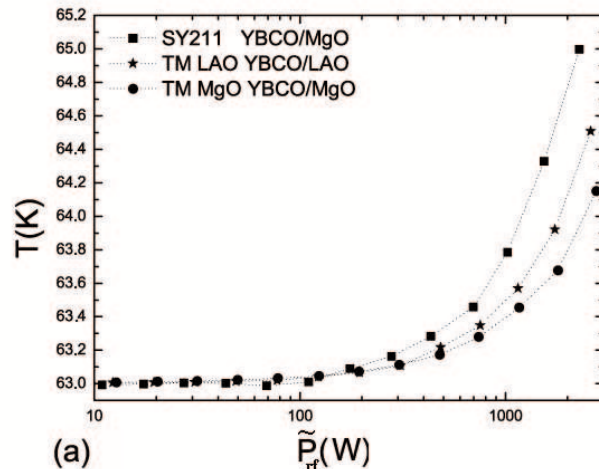
Kermorvant et al. Fig. 3



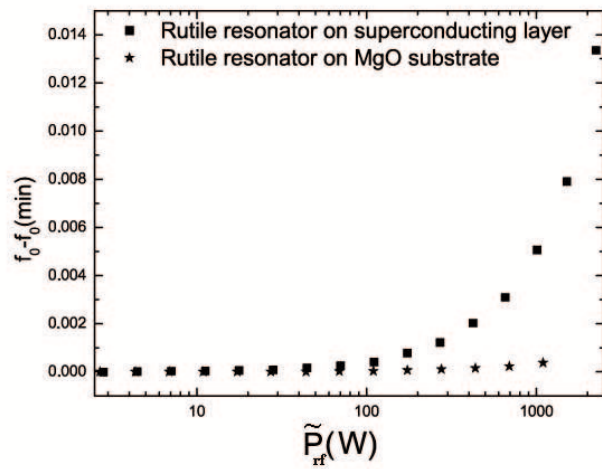
Kermorvant et al. Fig. 4



Kermorvant et al. Fig. 5



Kermorvant et al. Fig. 6



Kermorvant et al. Fig. 7